# Journal Pre-proof

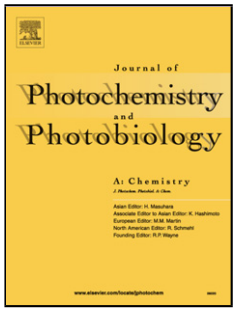


Fluorescent signal transduction in a self-assembled $Hg^{2+}$ chemosensor tuned by various interactions in micellar aqueous environment

Raimondo Germani, Paola Anastasio, Michele Chiodini, Tiziana Del Giacco, Matteo Tiecco, Leonardo Belpassi

PII: S1010-6030(19)31410-8

DOI: https://doi.org/10.1016/j.jphotochem.2019.112276

Reference: JPC 112276

To appear in: *Journal of Photochemistry & Photobiology, A: Chemistry*

Received Date: 16 August 2019

Revised Date: 5 November 2019

Accepted Date: 29 November 2019

Please cite this article as: Germani R, Anastasio P, Chiodini M, Del Giacco T, Tiecco M, Belpassi L, Fluorescent signal transduction in a self-assembled $Hg^{2+}$ chemosensor tuned by various interactions in micellar aqueous environment, *Journal of Photochemistry and amp; Photobiology, A: Chemistry* (2019), doi: https://doi.org/10.1016/j.jphotochem.2019.112276

# Fluorescent signal transduction in a self-assembled $Hg^{2+}$ chemosensor tuned by various interactions in micellar aqueous environment.

Raimondo Germani[a,b], Paola Anastasio[a], Michele Chiodini[a], Tiziana Del Giacco[a,b,*], Matteo Tiecco[a] and Leonardo Belpassi[c]

[a]*Dipartimento di Chimica, Biologia e Biotecnologie, Università di Perugia, Via Elce di Sotto 8, 06123 Perugia, Italy*

[b]*Centro di Eccellenza Materiali Innovativi Nanostrutturati (CEMIN), Università di Perugia, Via Elce di Sotto 8, 06123 Perugia, Italy*

[c]*Istituto di Scienze e Tecnologie Molecolari del CNR (CNR-ISTM), Università di Perugia, Via Elce di Sotto 8, 06123 Perugia, Italy*

[*]Corresponding author. Fax: +39 755855560.

E-mail addresses: tiziana.delgiacco@unipg.it (T. Del Giacco)

**Graphical abstract**

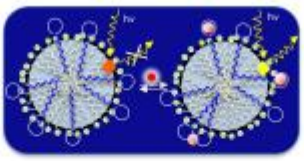

## Highligths:

- Assembly of acridinium perchlorate with an aza-thioether by micelles as a new $Hg^{2+}$ sensor is focused.
- The fluorescent transduction signal depends on stoichiometry of the aza-thioether -$Hg^{2+}$ complex.
- The operating switching mechanism is supposed to be a photoinduced electron transfer process.

**Abstract**

A new OFF-ON fluorescent chemosensor for ions $Hg^{2+}$ in water has been designed by associating fluorophore 10-methylacridinium perchlorate (**$MA^+ClO_4^-$**) with a selective lipophilic sulfur-containing ligand, such as N,N-bis (2-hydroxyethylthio-1-ethyl)dodecyl amine (**DBSO**). The communication between the two subunits is only due to their spatial closeness, ensured by sodium dodecyl sulfate (SDS) micellar aggregates. The quenching of **$MA^+$** fluorescence is ascribed to a photoinduced electron-transfer from the ligand to the excited fluorophore, still the emission is

quickly restored by addition of $Hg^{2+}$ (as chloride salt) due to the complex formation between ligand and metal. The sensitivity of the system improves by decreasing the ligand concentration, as well as by changing the stoichiometry of the ligand-$Hg^{2+}$ complex from 1:1 to 2:1. DFT calculations give interesting insights into the structures of the complexes and provide useful information on the sensorial activity experimentally observed. The replacement of **$MA^+ClO_4^-$** with 9-cyanoanthracene, a fluorophore differently localized on the micellar aggregate, highlights the effect of $Cl^-$ coordination to the complexed $Hg^{2+}$ on the operating mechanism of the sensor. These results demonstrate as the micellar aggregates provide for a straightforward means to regulate the response of the sensorial system without altering the recognition or reporter unit.

Keywords: self-assembling, fluorescent sensor, micellar aggregate, photoinduced electron transfer, complex stoichiometry

## 1. Introduction

The development of self-assembled fluorescent chemosensors has been attracting considerable attention in recent years. New efficient strategies have been developed to overcome the synthetic difficulty of connection between the two main components of a fluorescent sensor, namely receptor and fluorophore [1–3]. One of these implies the molecular organization of the sensor components into a supramolecular assembly, which provides close proximity between the active components, producing systems with new features. Actually, the possible insertion of lipophilic species inside hydrophobic core of surfactant aggregates, or binding of ionic species at the oppositely charged micellar surface, displays great capacity to establish the communication among the active species (i.e., fluorophore, receptor and analyte) in pure aqueous medium. The association of the active components of sensorial systems inside micellar nanostructures has been explored in order to design

new classes of fluorescent chemosensors with sensitivity and selectivity that are competitive with those of existing linked sensors [4–11].

In a previous work, we have exploited the self-assembling strategy for the realization of an off-on fluorescent PET (photoinduced electron transfer) sensor for $Hg^{2+}$ [6], one of the most toxic heavy metal ions for the environment and health [12,13]. This study was finalized to rationalize if the nature of the components, in terms of hydrophilic/lipophilic balance, was able to tune the sensing property of the sensor system in the $Hg^{2+}$ detection. Following this strategy, considering the growing demand in highly sensitive and selective detection of trace concentration of $Hg^{2+}$ in the environment and physiological media [14-17], we have sought to develop a sensorial system that provides easy detection of the analyte at a largely sensitivity level. For this purpose, in the present study we have described the properties of associating an efficient fluorescent reporter (cationic: 10-methylacridinium perchlorate, **$MA^+ClO_4^-$**, and non-ionic: 9-cyanoanthracene, **CA**, Scheme 1) and a lipophilic sulfur-containing ligand (N,N-bis (2-hydroxyethylthio-1-ethyl)dodecyl amine, **DBSO**, Scheme 1), which selectively binds soft $Hg^{2+}$ ions. Both fluorophores were selected for the following reasons: (i) the excellent fluorescence and electrochemical properties permit a high sensitivity [18,19], and (ii) the fluorescence properties are not altered by $Hg^{2+}$ [20]. In water, the relatively lipophilic ligand and fluorophore molecules move into SDS inert aggregates to generate a supramolecular assembly able to detect metal ion concentration well below the micromolar range. The results herein described emphasize how the fluorophore/receptor molar ratio affects the sensitivity of the sensorial system, as well as the stoichiometry of the **DBSO**-$Hg^{2+}$ complex. Moreover, the non-ionic and charged nature of two fluorophores, which determines a different interaction with the micellar pseudo-phase, and their different photophysical and electrochemical properties play a fundamental role as regards the sensor performance. The transduction is based on the enhanced fluorescence consequently to the **DBSO**-$Hg^{2+}$ interaction, supposedly owing to the preclusion of PET process between the excited fluorophores and the receptor. This has allowed the realization of a more desirable “turn-on” sensor to achieve high selectivity [21]. The results of this

study have been integrated by DFT (Density Functional Teory) calculations in order to obtain information on the geometry of the Hg-receptor complexes. This information was useful to better support the implication of 1:1 and 2:1 (ligand:$Hg^{2+}$) complexes in the sensing mechanism switching.

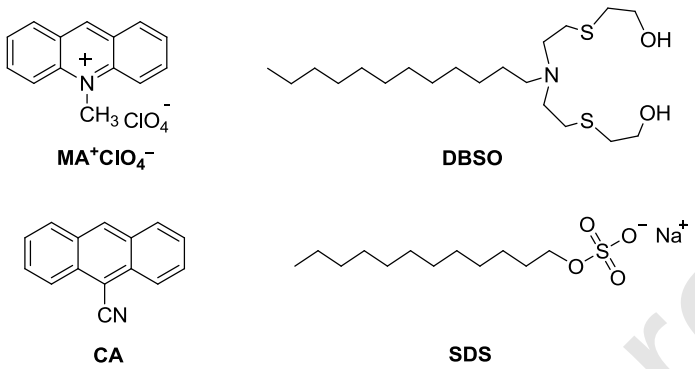


**Scheme 1.** Molecular structures of fluorophores **$MA^+ClO_4^-$** and **CA**, receptor **DBSO** and surfactant SDS.

## 2. Experimental

### *2.1 Instrumentation and materials*

Absorption spectra were recorded on an Agilent 8453 Diode Array UV-Vis spectrophotometer. Fluorescence emission spectra were measured with a BioTek Synergy H1 Hybrid Multi-Mode Microplate Reader spectrometer. $^1$H NMR spectra were recorded on a Bruker Avance III HD 400 MHz Smart Probe spectrometer (400 MHz for $^1$H NMR) and were internally referenced to the residual proton solvent signal.

The organic solvents were of HPLC grade. Milli Q water (18 MΩ, pH 6.50) was used for all spectroscopic measurements. The measurements were carried on unbuffered aqueous solutions. Commercially available SDS (Sigma-Aldrich) was recrystallized twice from an acetone–methanol mixture before using [22]. All the chloride salts of $Hg^{2+}$, $K^+$, $Mg^{2+}$, $Ca^{2+}$, $Mn^{2+}$, $Ni^{2+}$, $Cu^{2+}$, $Zn^{2+}$, $Cd^{2+}$, and $Al^{3+}$ions and nitrate and perchlorate salts of $Ag^+$, $Pb^{2+}$ and $Mg^{2+}$, respectively, purchased from commercial suppliers, were of analytical reagent grade and used after drying. All the other

reagents were obtained from commercial suppliers and used as received. **$MA^+ClO_4^-$** was synthesized from acridine by quaternization with methyl iodide in acetonitrile and subsequent ion exchange by sodium perchlorate in methanol [23]. Spectral data of **$MA^+ClO_4^-$** are in accordance with literature data [24]. Receptor **DBSO** was synthesized in three steps following procedures already known. Firstly, N,N-bis(2-hydroxyethyl)dodecylammonium chloride was prepared by alkylation of bis(2-hydroxyethyl)amine with dodecyl bromide and then converted in N,N-bis(2-chloroethyl)dodecylammonium chloride by reaction with thionyl chloride in anhydrous dichloromethane [25,26]. In the last step, amine hydrochloride (13 mmol), 2-hydroxy-1-ethanethiol (29 mmol) and $K_2CO_3$ (39 mmol) were placed in a round bottom flask fitted with a reflux condenser and then mixed in 200 mL of acetonitrile. The mixture was magnetically stirred at 75 °C for 24 h under nitrogen; after cooling, $K_2CO_3$ was filtered off and the solvent was removed under reduced pressure to yield a yellow oil. The product was purified by column chromatography (silica gel) using diethyl ether as eluent to give a pale yellow liquid (60 % yield). $^1$HNMR ($CDCl_3$, 400 MHz): δ 3.77-3.75 (m, 4H, -$CH_2$OH), 277-268 (m, 12H, -$NCH_2CH_2SCH_2$-), 2.53-2.50 (m, 2H, N-$\underline{CH_2}$-$(CH_2)_{10}CH_3$); 1.47 (s broad, 2H, $NCH_2\underline{CH_2}(CH_2)_9CH_3$); 1.27 (s, 18H, $NCH_2CH_2(\underline{CH_2})_9CH_3$); 0.89 (t, 3H, N-$(CH_2)_{11}\underline{CH_3}$).

*2.2 Photophysical measurements*

All spectrophotometric and spectrofluorometric analyses of the fluorophore/receptor/metal systems were performed in 0.010 M SDS aqueous solutions at 25.0 °C. The stock solutions of fluorophores **$MA^+ClO_4^-$** ($1.0 \times 10^{-3}$ M), **CA** ($1.0 \times 10^{-3}$ M) and receptor **DBSO** (0.1 M) were prepared in water, acetonitrile and ethanol, respectively. The stock solutions of metal ions and solutions diluted by these were prepared in aqueous solution. Diluted surfactant solutions of fluorophore and receptor were prepared about 24 hours before spectroscopic measurements, so that the components had the time to equilibrate between the aqueous bulk and the micellar aggregates. Acridinium and cyanoanthracene concentrations were kept $5.3 \times 10^{-6}$ and $5.0 \times 10^{-6}$ M, respectively,

in all solutions; this allowed an absorbance < 0.1 at the excitation wavelength (359 and 365 nm, respectively), necessary to avoid self-absorption effects. Generally, the UV-Vis absorption and fluorescence titrations were performed by the gradual addition of the metal ion stock solution into 3.2 ml of fluorophore/receptor surfactant solution in a quartz cuvette with 1 cm optical path. All solutions were mixed carefully before measurements.

*2.3 Computational details*

The geometry optimizations were computed with the ADF package (version 2016.104) at the density functional theory (DFT) level using TZ2P Slater-type basis sets [27], Becke's exchange functional in combination with the Lee − Yang − Parr correlation functional [28,29], frozen-core approximation and ZORA Hamiltonian to account relativistic effects [30-32]. We employed the numerical integration grid with precision 6.0 (Table S1). All of the studied geometries that have been optimized are local minima.

## 3. Results and discussion

*3.1. Spectrophotometric titration of **DBSO** with $Hg^{2+}$ in SDS micelle solutions.*

The interaction of **DBSO** with $Hg^{2+}$ was first studied by UV-spectroscopy in the absence of fluorophore to determine the intrinsic behavior of the receptor. The spectrophotometric titration of **DBSO** ($1.0 \times 10^{-4}$ M) upon mixing with $Hg^{2+}$ ($0 - 3.34 \times 10^{-4}$ M) in 0.010 M SDS solution was reported in Fig. 1. The SDS concentration was maintained higher than its critical micellar concentration ($8.0 \times 10^{-3}$ M in pure water [33], but it could be lower in the presence of electrolyte) in all the experiments. The addition of increasing amounts of metal ions clearly led to a batochromically shifted absorption around 240 nm, as well as an increase of absorbance up to $\sim 1 \times 10^{-4}$ M $Hg^{2+}$ (concentration equal to that of **DBSO**), which was assigned to the **DBSO**-$Hg^{2+}$ complex formation.

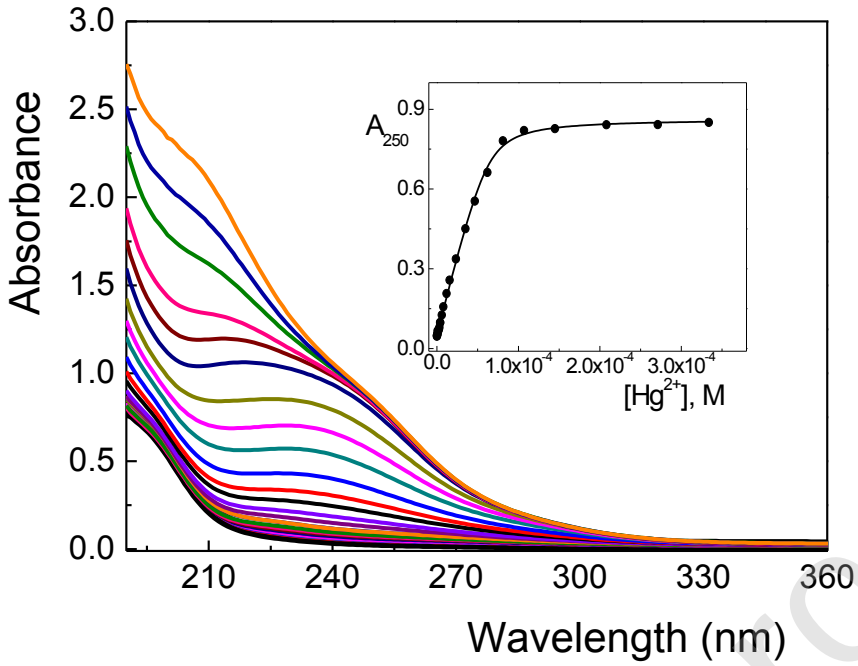


**Fig. 1.** Absorption spectra of **DBSO** ($1.0 \times 10^{-4}$ M) alone (black line) and recorded in the presence of various $Hg^{2+}$ concentrations ($7.81 \times 10^{-8}$ – $3.34 \times 10^{-4}$ M) in 0.010 M SDS solution. Inset: change in absorbance at 250 nm ($A_{250}$) as a function of [$Hg^{2+}$].

The interaction of the ligand with $Hg^{2+}$ ions should be mainly located near the sulfur and nitrogen atoms of the chelating region, being these atoms softer than oxygen and therefore more incline to interact with the soft $Hg^{2+}$ ions [34,35]. At $Hg^{2+}$concentration close to that of **DBSO** ($\sim 1 \times 10^{-4}$ M), no further absorbance increase at $\lambda > 240$ nm was observed, in line with the complete complexation of the ligand. The absorption continued to enhance only at wavelengths below 240 nm, assigned to the mercury aquo complex by comparison with the absorption spectra recorded, in the absence of receptor, upon addition of $Hg^{2+}$ ($1.67 \times 10^{-7}$ – $3.36 \times 10^{-4}$ M) in aqueous SDS solution (Fig. S1 in the Supplementary Information). By plotting the absorbance at 250 nm (wavelength where only **DBSO**-$Hg^{2+}$ complex absorbed), as a function of [$Hg^{2+}$] (insets in Fig. 1), a break point was highlighted at 1 equivalent of $Hg^{2+}$, providing evidence for a 1:1 binding stoichiometry. The complexation constant (*K*), determined according to the procedure previously described [6], was found to be $2.7 \times 10^5$ $M^{-1}$. As observed in Fig. S2, a satisfactory fitting curve by Eq. (1) (where $A_0$ is

for absorbance without metal, $A_{lim}$ is the limit value when the ligand is fully complexed, [$Hg^{2+}$] and [**DBSO**] refer to the analytical concentrations of the metal and ligand, respectively) was found, with correlation coefficient of 0.9990, endorsing the 1:1 stoichiometry of the complex.

$$A = A_0 + \frac{A_{lim} - A_0}{2[DBSO]} \{[DBSO] + [Hg^{2+}] + 1/K - (([DBSO] + [Hg^{2+}] + 1/K)^2 - 4[DBSO][Hg^{2+}])^{0.5}\} \quad (1)$$

Taking into account that the sensorial system was examined with **DBSO** both at $1.0 \times 10^{-4}$ and $3.0 \times 10^{-4}$ M (see below), the changes in the absorption spectra of a more concentrated receptor solution ($3.0 \times 10^{-4}$ M) mixed with $Hg^{2+}$ ($1.35 \times 10^{-7} - 9.89 \times 10^{-5}$ M) in SDS solution were also recorded (Fig. S3). In this case, a plateau value was not achieved, since the spectra were recorded up to 0.3 equivalents of $Hg^{2+}$; anyway, a good fitting of absorbance at 250 nm vs. [$Hg^{2+}$] data by eq (1) was observed (Fig. S4), confirming the formation of the **DBSO**-$Hg^{2+}$ complex with *K* value of $2.3 \times 10^5$ $M^{-1}$ (correlation coefficient = 0.9976), value close to that calculated at **DBSO** lower concentration.

*3.2 Cation-induced changes in photophysical properties of the **MA**$^+$**/DBSO** system in SDS micelles*

As is evident in Fig. 2, the fluorescence emission intensity ($\lambda_{max}$ = 495 nm) of a SDS solution of **MA**$^+$ ($5.3 \times 10^{-6}$ M, kept constant in all experiments) was first quenched of 48% by addition of $1.0 \times 10^{-4}$ M **DBSO** (black and green line, respectively) and then was turned back with gradual addition of $Hg^{2+}$ ions, without an appreciable shift in the emission maximum. At the excitation wavelength used only the fluorophore absorbed (see absorption spectra of **MA**$^+$ and **DBSO** in Fig. S5). A plateau level was reached after titration by ~ 1 equivalent of mercury ions with respect to the receptor moles (see inset in Fig. 2). The fact that adding $1.0 \times 10^{-4}$ M $Hg^{2+}$ to the system in the absence of **DBSO** resulted in a fluorescence quenching of just 1% (see Fig. S6) indicated that the interaction between receptor and metal is indeed required for signal generation.

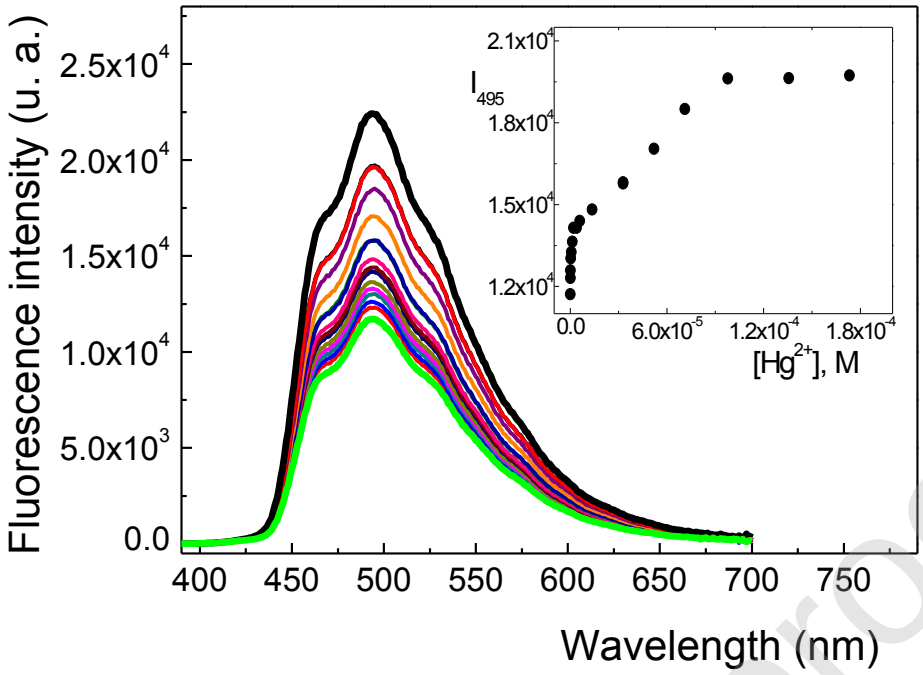


**Fig. 2.** Fluorescence emission spectra of $5.3 \times 10^{-6}$ M **MA**$^+$ alone (black line), in the presence of $1.0 \times 10^{-4}$ M **DBSO** (green line) and various $Hg^{2+}$ concentrations ($7.81 \times 10^{-8} - 1.73 \times 10^{-4}$ M) in 0.010 M SDS solution; $\lambda_{exc}$ = 359 nm. Inset: change in intensity at 495 nm ($I_{495}$) as a function of [$Hg^{2+}$].

Thanks to the modular nature of the self-assembling sensor system in micellar medium, it was possible to point out the effect of the receptor concentration on the fluorescence behavior of the system, and so to tune the detection range just by the modification of the component ratio. Indeed, for sensorial system **MA**$^+$/**DBSO**, spectrofluorimetric titrations carried out at higher concentrations of receptor with $Hg^{2+}$ ions exhibited a similar spectral behavior, as observed in Fig. S7 and Fig. S8 and corresponding insets, where the plots of the fluorescence emission at concentration of $1.5 \times 10^{-4}$ and $5.0 \times 10^{-4}$ M receptor, respectively, are shown. For the sake of comparison, the $I_{495}$ versus [$Hg^{2+}$] profiles at all the investigated concentrations of **DBSO** are collected in Fig. 3. An evidence is that the quenching fluorescence percentage of **MA**$^+$, calculated with respect to the fluorescence of **MA**$^+$ alone (indicated by open circle symbols in Fig. 3), dropped from 48 % in the presence of $1.0 \times 10^{-4}$ M **DBSO** to 67 and 91 % for $1.5 \times 10^{-4}$ and $5.0 \times 10^{-4}$ M **DBSO** solution, respectively. This suggests that the electron transfer from **DBSO** to **MA**$^+$ excited state [36], reaction assumed

plausible on the basis of their redox potentials ($E_{ox}$ = 0.94 V vs. SCE in $CH_3CN$ approximate equal to that of triethylamine [37]; $E^*_{red}$ = 2.32 V vs. SCE in $CH_3CN$ [18]) becomes more and more efficient. This result is expected considering that the fluorophore, being charged, may be located in the micelle-water interface (about 1 every 6 micelles, being $3 \times 10^{-5}$ M the average micellar concentration at the surfactant analytical concentration of 0.010 M [6]); accordingly, it will be surrounded by an increasing number of ligands, equal to 3, 5, 17, with $1.0 \times 10^{-4}$, $1.5 \times 10^{-4}$ and $5.0 \times 10^{-4}$ M **DBSO**, respectively, suitable to turn off the acridinium fluorescence. The fluorescent enhancement observed at all the **DBSO** concentrations in the presence of $Hg^{2+}$ plausibly arise from the metal coordination to the receptor chelating region, which removes in particular the amino nitrogen of **DBSO** as the source responsible for the intermolecular quenching. Reasonably, the $Hg^{2+}$-amine interaction drops the lone pair energy, increasing oxidation potential, accordingly the PET is less efficient. The emission intensity of $\mathbf{MA}^+$ turned on upon addition of $Hg^{2+}$, reaching a maximum value at ~ 1 equivalent of metal, both at $1.5 \times 10^{-4}$ and $5.0 \times 10^{-4}$ M of **DBSO** (Fig. S7 and Fig. S8, respectively) as already observed at lower receptor concentration.

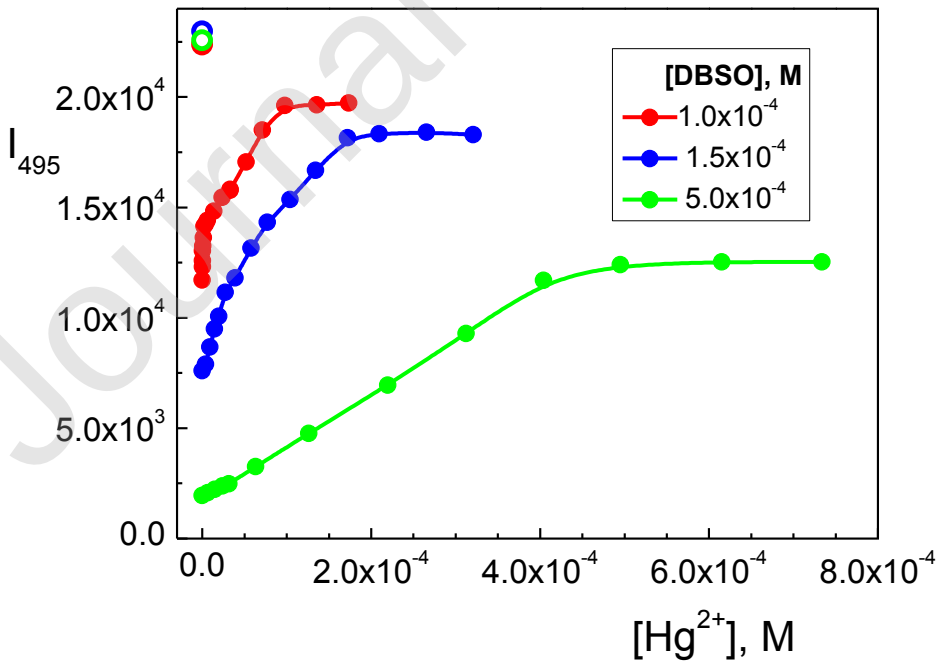

**Fig. 3.** Change in intensity at 495 nm ($I_{495}$) as a function of $Hg^{2+}$ concentration of **MA**$^+$ ($5.3 \times 10^{-6}$ M) in the presence of $1.0 \times 10^{-4}$ M (●), $1.5 \times 10^{-4}$ M (●) and $5.0 \times 10^{-4}$ M (●) **DBSO** in 0.010 M SDS solution; symbols ⭘, ⭘, ⭘ represent $I_{495}$ of **MA**$^+$ alone**.**

Another important aspect of the profiles depicted in Fig.3 is the fluorescence enhancement below 100% in all the examined cases; this means that the PET was not sufficiently suppressed by mercuric ion binding. The restored fluorescence percentage, calculated with respect to the fluorescence of **MA**$^+$ alone, decreased by increasing **DBSO** concentration (with values of 88, 80 and 55 %), in line with the increase in efficiency of the PET process (see above). An explanation of such behavior could be that four of the five ligating centers (two sulfurs and two oxygens) do not contribute directly to remove the PET, rather they compete negatively by dispersing a fraction of the ionic charge [38].

A very interesting feature of our system was that to show a significant increase in fluorescence intensity ($I_{495}$) already upon addition of $Hg^{2+}$ in the micro and submicromolar range of concentration (Fig. 3). Specially, in the presence of $1.0 \times 10^{-4}$ M **DBSO**, plot $I_{495}$ as a function of $Hg^{2+}$ concentration was clearly nonlinear at metal concentration lower than 1 equivalent, contrary to what was observed by UV/vis titrations (Fig. 1). These experiments suggest that a ternary complex **DBSO**-$Hg^{2+}$-**DBSO** is selectively formed upon addition of lower concentrations of $Hg^{2+}$, which only a fluorescence signaling technique is able to detect because of its high sensitivity. The ability of sulfide derivative ligands to form 2:1 (ligand:metal) complexes with mercuric ions is however well known [39–41]. Further addition of metal (higher than 2 μM) favored the formation of complex **DBSO**-$Hg^{2+}$ (1:1 binding stoichiometry), already rationalized by UV/vis investigation, that led to a worse sensitivity of the sensor, as emphasized by the data shown in Fig. 3. The reason of the more efficient ability of the 2:1 complex with respect to the 1:1 complex to remove the PET process was researched by analyzing the geometry of the two structures. Thus, for a meaningful discussion of the experimental results, DFT calculations were performed in gas phase for molecular simulation of the geometrical structure of the complexes that the aza-thioether (with methyl instead

of dodecyl tail to simplify the calculation, named **DBSO'**) forms with $Hg^{2+}$ ions. Fig. 4 depicts DFT-optimized structures for the most stable conformers of complexes (**DBSO'-Hg**)$^{2+}$ and (**DBSO$_2$'-Hg**)$^{2+}$. Bond distances of interest are given in Table 1. The 1:1 complex was predicted to present an almost linear coordination around the metal ion, with a Hg–S distances of 2.52 and 2.48 Å. Conversely, the $Hg^{2+}$ complexed with two receptor molecules showed a distorted tetrahedral coordination, with four S atoms from the **DBSO'** ligands bonded to the Hg atom, with similar Hg–S bond distances for a ligand (2.82 and 2.83 Å) and quite different for the other one (2.61 and 2.79 Å). Therefore, the $Hg^{2+}$ complexes tend to be distorted by the formation of short bonds to more covalently bound donor atoms, such as sulfur, and longer bonds to more ionically bound donor atoms, as nitrogen and oxygen (see Table 1). The preferential bonding of $Hg^{2+}$ ion to soft sulfur-based ligands is in line with the HSAB (hard and soft acids and bases) classification [42]. The trend between Hg(II)–S bond distance and Hg(II) coordination number was the same as observed for the series of mononuclear thiolate complexes, $Hg(SR)_n$ [43]. Interestingly, the geometric distortion of the second ligand should lead to the intramolecular hydrogen bonding interaction (depicted by an oval frame in Fig 4b) between the hydroxyl and the nitrogen atom of **DBSO'** molecule, which is peculiar only of complex **(DBSO$_2$'-Hg)**$^{2+}$. The hydrogen bond length of 1.75 Å, quite shorter than the averaged hydrogen bond distance in water (1.88 Å, in standard condition of pressure and temperature [44]) highlights a significant bond strength. We hypothesize that just this hydrogen interaction in the 2:1 complex, able to remove the PET from the donor nitrogen atom to excited **MA**$^+$, is responsible for the greater sensitivity of the sensor.

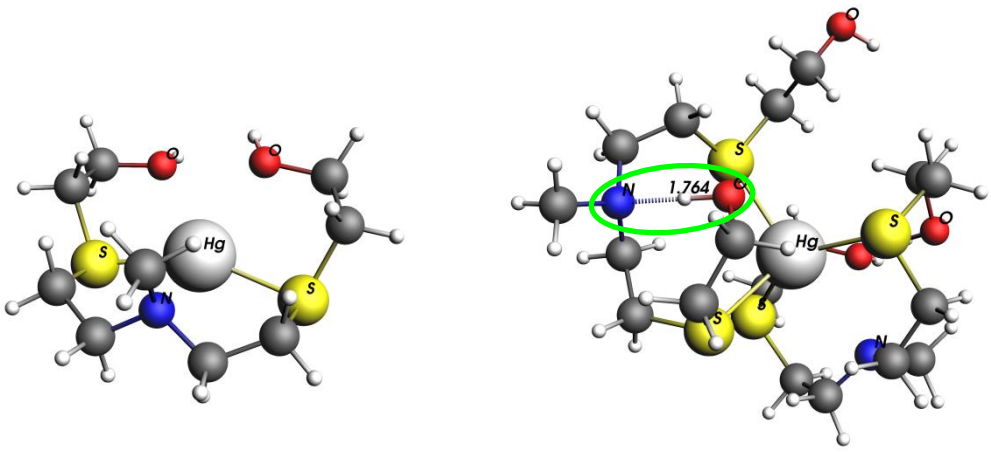


**(a)** **(b)**

**Fig. 4.** Optimized structures of complexes **(DBSO'-Hg)$^{2+}$** (a) and **(DBSO$_2$'-Hg)$^{2+}$** (b) (C = grey; O = red; H = white; S = yellow).

**Table 1**
Optimized Hg-X (with X=S, N, O) bond distances for complexes **(DBSO'-Hg)$^{2+}$** .and **(DBSO$_2$'-Hg)$^{2+}$**.[a]

| Complex | d(Hg-S) | d(Hg-N) | d(Hg-O) |
|---|---|---|---|
| **(DBSO'-Hg)$^{2+}$** | 2.52, 2.48 | 2.57 | 2.50, 3.13 |
| **(DBSO'$_2$-Hg)$^{2+}$** | 2.61, 2.79, 2.82, 2.83 | 2.98, 4.01 | 3.72, 4.03, 5.58, 2.89 |

[a]Values, in Å, obtained at BLYP/TZ2P level using the scalar ZORA Hamiltonian.

Another intriguing evidence was that in the micromolar concentration range, plot $I_{495}$ versus [$Hg^{2+}$] became more linear by increasing **DBSO** concentration, in parallel to a decrease of sensitivity (Fig. 3). Indeed the slopes of the response curves, revealed that the signal change induced by the same amount of $Hg^{2+}$ (4 μM) was *ca.* 10 and 50 times stronger at $1.0 \times 10^{-4}$ M **DBSO** compared to $1.5 \times 10^{-4}$ and $5.0 \times 10^{-4}$ M **DBSO**, respectively. Therefore, the sensitivity decreases with the dilution of $Hg^{2+}$ with respect to the receptor molecules in the micellar aggregates, as it increases the probability that ions $Hg^{2+}$ bind to receptors associated with micelles devoid of fluorophore [21,45].

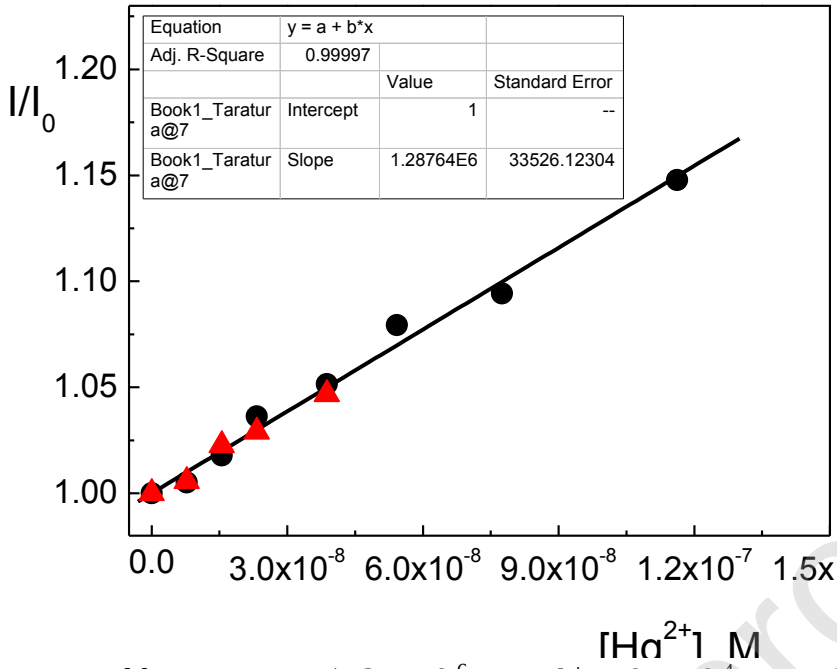


**Fig. 5.** Fluorescence calibration curve ($5.3 \times 10^{-6}$ M **MA**$^+$, $1.0 \times 10^{-4}$ M **DBSO** in 0.010 M SDS solution, λ = 495 nm) used for the sensor assay in the $Hg^{2+}$determination by linear plotting method ($I_0$ e $I$ are the intensities of **MA**$^+$ in the presence of **DBSO** without and with $Hg^{2+}$, respectively); (●)18 MΩ Milli Q water and (▲) tap water.

In optimal sensitivity condition, i. e. at [**DBSO**] = $1.0 \times 10^{-4}$ M**,** the system was able to generate an excellent linear response curve reported as $I/I_0$ ratio (where $I$ and $I_0$ refer to the intensity with and without $Hg^{2+}$, respectively) as a function of $Hg^{2+}$ concentration in the nM concentration range (Fig. 5). For this purpose, a set of known various standard solutions of $Hg^{2+}$ (8−120 nM), prepared as described in Experimental Section, were measured and the calibration plot was established by $I/I_0$ ratio determination at 495 nm. The detection limit, calculated by the $3\sigma s^{-1}$ relationship, where σ = standard deviation of blank response and s = slope of the linear regression, was found 22 nM (against 2.0 μM and 16 μM at $1.5 \times 10^{-4}$ and $5.0 \times 10^{-4}$M **DBSO**, respectively), somewhat lower with that observed for other $Hg^{2+}$-sensing systems based on the same motif [46,47]. A response to [$Hg^{2+}$] in the nM range was measured in real water samples (tap water). For this purpose, the tap water sample solutions were prepared and the response percentage was of 98-100 % compared with those in pure water, proving the sensing system tolerance to the presence of other components (Fig. 5).

As regards the selectivity of the sensing system, it was evaluated by a comparative study among a series of 10 metal ions (such as $K^+$, $Mg^{2+}$, $Ca^{2+}$, $Mn^{2+}$, $Ni^{2+}$, $Cu^{2+}$, $Zn^{2+}$, $Ag^+$, $Cd^{2+}$, and $Al^{3+}$) at a constant concentration of $1.0 \times 10^{-5}$ M (Fig. 6).

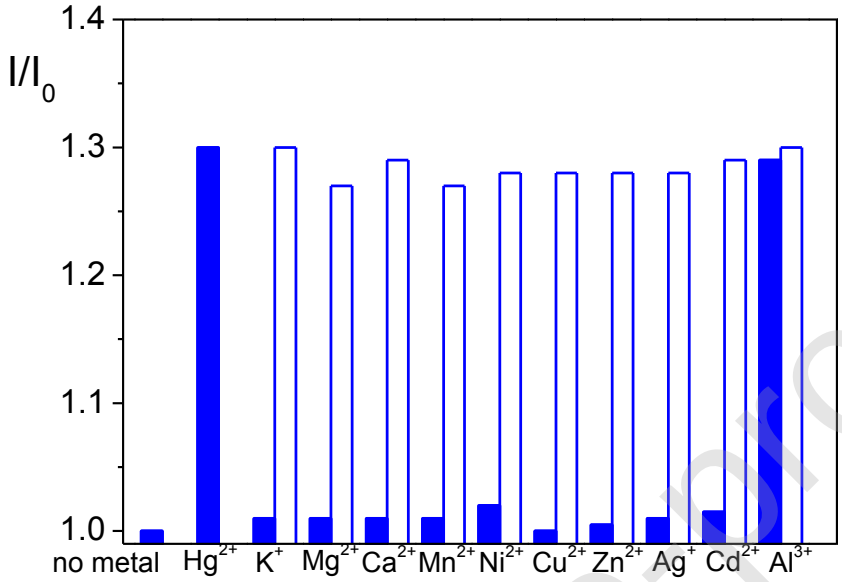


**Fig. 6.** Plot of $I/I_0$ (where $I$ and $I_0$ refer to the intensity of the **MA**$^+$ ($5.3 \times 10^{-6}$ M)/**DBSO** ($1.0 \times 10^{-4}$ M) system in the presence and absence of metal ion, respectively, at 495 nm) recorded in 0.010 M SDS solution upon addition of $Hg^{2+}$ ($1.0 \times 10^{-6}$ M) and various cations ($1.0 \times 10^{-5}$ M), full bars. Not filled bars represent $I/I_0$ of **MA**$^+$ with **DBSO** in the presence of the indicated metal ions, followed by addition of $1.0 \times 10^{-6}$ M $Hg^{2+}$.

Except $Al^{3+}$, only for $Hg^{2+}$ ($1.0 \times 10^{-5}$ M) a significant increase in $I/I_0$ ratio was observed, indicative of the inability of other metal ions to form a complex with **DBSO**. By competition experiments, carried out under identical conditions, fluorescence intensity was restored in the presence of $Hg^{2+}$ ($1.0 \times 10^{-6}$ M) with all the metal ions examined. However, $Al^{3+}$ was a significant interferent for the mercury detection. We also performed a spectrophotometric titration (Fig. S9) with $Al^{3+}$, in the absence of **MA**$^+$, and we compared the results with that obtained with $Hg^{2+}$. Correlation of the spectrophotometric data ($A_{280}$ versus [$Al^{3+}$], see inset of Fig. S9) by Eq. (1) consisting with the 1:1 complex model, allowed us to valuated a conditional $K$ value of $5.8 \times 10^4$ $M^{-1}$. Thus, a stability constant of complex **DBSO**-$Al^{3+}$ only 5 times smaller than that obtained for **DBSO**-$Hg^{2+}$, together

with an enhancement of the "metal sponge effect" due to a stronger electrostatic interaction between the anionic micellar surface and the more densely charged $Al^{3+}$, make the selectivity of this system towards $Hg^{2+}$ not so good over $Al^{3+}$.

*3.3 Cation-induced changes in photophysical properties of the **CA**/**DBSO** system in SDS micelles*

An intriguing scenario was observed when $Hg^{2+}$ titrations were performed in the presence of fluorophore **CA**. The fluorescence experiments, performed exciting selectively $5.0 \times 10^{-6}$ M **CA** at 365 nm in 0.010 M SDS (absorption spectrum in Fig. S10), showed a lowering of the emission intensity (maximum at 448 nm) when the **DBSO** amount increased from $1.0 \times 10^{-4}$ to $3.0 \times 10^{-4}$ M (Fig. S11), as already observed in similar experiments using $\mathbf{MA^+}$ as a fluorophore. In particular, the intensity was reduced of 13 and 31% of its initial value at $1.0 \times 10^{-4}$ and $1.5 \times 10^{-4}$ M **DBSO**, respectively, against 48 and 67% obtained with $\mathbf{MA^+}$ at the same receptor concentrations. The PET suppression therefore seems less effective with **CA**, most likely due to its lower reduction potential in the singlet excited state ($E^*_{red}$ = 1.46 V vs. SCE in $CH_3CN$ [19]). In the presence of $3.0 \times 10^{-4}$ M **DBSO,** the initial fluorescence enhancement of **CA** accompanying the mercury complexation of **DBSO** plausibly removes the amine group from the electron transfer with the excited fluorophore (Fig. S12). Curiously, for $Hg^{2+}$ concentrations higher than ca. $6 \times 10^{-5}$ M, a gradual decrease of the fluorescence was instead observed up to $1.15 \times 10^{-4}$ M (Fig. S13), never observed with $\mathbf{MA^+}$ as a fluorophore. The lack of a significant effect of mercuric ions (from $1.00 \times 10^{-7}$ to $2.00 \times 10^{-4}$ M, see Fig. S14) on the **CA** fluorescence emission in the absence of **DBSO** points out that the receptor metal complex formation plays a decisive role. As already observed with $\mathbf{MA^+}$**, t**he plot of $I/I_0$ at 448 nm displaced as a function of [$Hg^{2+}$] was clearly nonlinear (Fig. 7), exhibiting a much stronger response at [$Hg^{2+}$]/[**DBSO**] < 0.001 which was attributed to the formation of the ternary complex **DBSO**-$Hg^{2+}$-**DBSO,** though not expected on the basis of the UV/Vis titration (Fig. S3). The subsequent rapid change of slope upon addition of [$Hg^{2+}$] > $3 \times 10^{-7}$ M suggests possibly the

involvement of a 1:1 binding stoichiometry. However, as reported above (Fig. S3), the absorption spectra of $3.0 \times 10^{-4}$ M **DBSO** mixed with $Hg^{2+}$ from $1.35 \times 10^{-7}$ to $9.89 \times 10^{-5}$ M in SDS solution confirmed the formation of the **DBSO**-$Hg^{2+}$ complex.

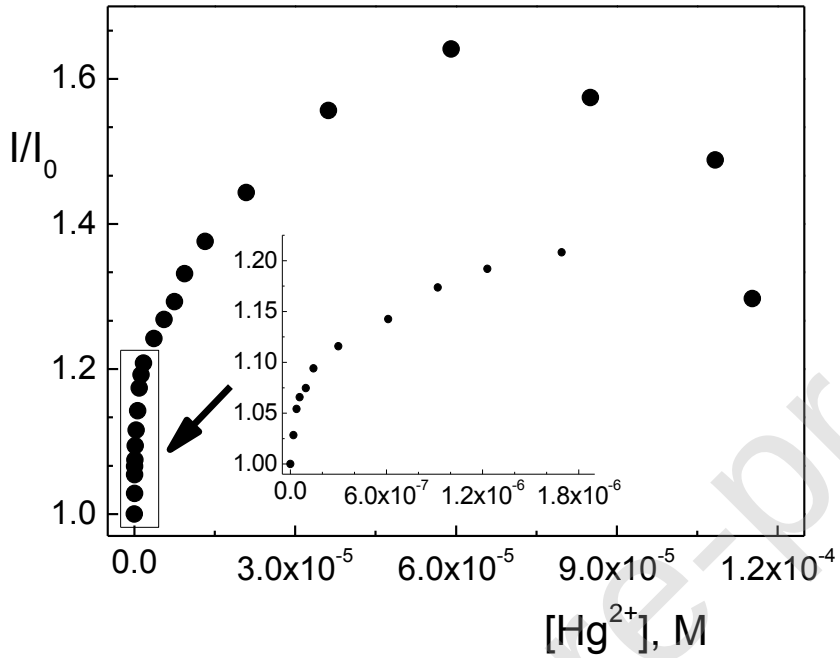


**Fig. 7** Plots of $I/I_0$ at 448 nm as a function of $Hg^{2+}$ concentration of **CA** ($5.0 \times 10^{-6}$ M) in the presence of $3.0 \times 10^{-4}$ M **DBSO** in 0.010 M SDS solution ($I$ and $I_0$ refer to the intensity with and without $Hg^{2+}$, respectively). Inset: enlargement of the $0 - 2 \times 10^{-6}$ M concentration range.

The visible fall in fluorescence at [$Hg^{2+}$]/[**DBSO**] higher than 0.2 clearly suggests that the PET process is not sufficiently suppressed by mercury binding anymore, likely due to a charge dispersal mechanism [38]. Specifically, the pairing ability of chloride anions to $Hg^{2+}$ coordinated with the receptor, leading to the **DBSO**-$HgCl_2$ complex formation, becomes significant at higher $Cl^-$ concentration in the micellar interface [48,49]. This effect should cause a weakening of the interaction of $Hg^{2+}$ with the **DBSO** amine group, thus allowing quenching by a PET mechanism. At this point one might wonder why with **CA** the fluorescence intensities passed through a maximum and fell off by increasing the $Hg^{2+}$ concentration, while with **MA**$^+$ reached a plateau level, although the same receptor was used (compare Fig. 7 with Fig. 3). In our opinion, such different behavior

may be rationalized taking into account that the self-assembly inside micelles involves the consequent selective compartmentalization of the fluorophore and the receptor, both free and bound to metal. We suppose the complex **DBSO**-$Hg^{2+}$, made more lipophilic when the $Hg^{2+}$ ion is further coordinated to two chloride anions, to be more included in the micelle lipophilic core, where also **CA**, being a hydrophobic fluorophore, should reside. This close proximity allows the ON-OFF fluorescence switching of the **CA**/**DBSO** system in the presence of $Hg^{2+}$, by a suitable charge perturbation, able to restore an efficient PET. On the contrary, the acridinium moiety is likely localized in the polar micelle-water interface (Stern layer), where the sulfate headgroups of surfactant interacts with the softer acridinium ions rather than with sodium ions. In this case the surfactant aggregates does not ensure the spatial closeness between fluorophore and complex **DBSO**-$Hg^{2+}$coordinated by chloride: the lipohilized ligand offers no quenching mechanisms, accordingly the fluorescence of $\mathbf{MA}^+$ is maintained in "ON" condition.

The narrow range of $Hg^{2+}$ concentrations, where the system CA/**DBSO** was able to generate a linear response curve, is responsible for its not excellent performance in terms of sensitivity. Selectivity study of CA/**DBSO** system was performed by recording the fluorescence spectra after the addition of each metal ions. Fig. S15 shows the dependence of $I/I_0$ as a function of cation concentration ($1.00 \times 10^{-7}$, $1.00 \times 10^{-6}$ and $1.00 \times 10^{-5}$ M) evaluated for all metals already tested with $\mathbf{MA}^+$ and in addition $Pb^{2+}$and $Fe^{3+}$. As already observed using $\mathbf{MA}^+$ as a fluorophore, only for $Hg^{2+}$ a significant increase in intensity ratio was detected, along with a relatively minor change in the emission by $Al^{3+}$ addition. Thus, as expected, the selectivity mainly was due to the ligand choice.

## 4. Conclusions

The fluorophore/probe system depicted here is designed for $Hg^{2+}$ ions and represents a new OFF-ON fluorescent chemosensor. SDS micelles allow the inter-component communication without the need for covalent linkage. This modular approach has allowed the easy change of the

fluorophore, the use of pure water instead of prevalently organic solvent mixtures, in addition to a high solubility of the components. A tuning of the sensor sensitivity can be easily obtained by changing the ligand to fluorophore ratio, without altering the recognition or reporter unit. Thus, the receptor concentration acts as a regulatory element that determines the effectiveness at which the presence of $Hg^{2+}$ is transduced into signal. The main novelty of this work is that the interaction of $Hg^{2+}$ with **DBSO** allows to modulate the strength of the output signal simply by changing the stoichiometry of the complexes between metal and receptor. The explanation of this experimental evidence is supported by DFT computations. An additional feature is that coordination of $Hg^{2+}$ to covalently binding ligands, such as $Cl^{-}$, tends to weaken the interaction of mercury with the **DBSO** N-donor, thus allowing quenching by PET. This occurs specially in the presence of a more hydrophobic florophore, such as **CA,** and at higher concentrations of mercuric chloride. Therefore, the signal transduction gives rise to response curves that are different from those typically observed in both self-assembled and bonded sensorial systems. Despite the complexity of our system, generated by assembly of three components, its performance in tap water has shown good reproducibility compared to that performed in deionized water. This proves that the application of this type of systems is a practicable way.

**Acknowledgments**

Thanks are due to the University of Perugia (Fondo Ricerca di Base 2018) for financial support.

**References**

[1] J. Wu, B. Kwon, W. Liu, E. V. Anslyn, P. Wang, J. S. Kim, Chromogenic/fluorogenic ensemble chemosensing systems, Chem. Rev. 115 (2015) 7893-7943.

[2] F. Mancin, E. Rampazzo, P. Tecilla, U. Tonellato, Self-assembled fluorescent chemosensors, Chem. Eur. J. 12 (2006) 1844–1854.

[3] T. Del Giacco, R. Germani, G. Lucci, M. Tiecco, Acid-base responsive probes for mercury(II) ions in aqueous solution, Microchem. J. 141 (2018) 127–134.

[4] N. Dey, S. Bhattacharya, A glimpse of our journey into the design of optical probes in self-assembled surfactant aggregates, Chem. Rec. 16 (2016) 1934-1949.

[5] P. Pallavicini, Y. A. Diaz-Fernandez, L. Pasotti, Micelles as nanosized containers for the self-assembly of multicomponent fluorescent sensors, Coord. Chem. Rev. 253 (2009) 2226-2240.

[6] T. Del Giacco, R. Germani, F. Purgatorio, M. Tiecco, Role of anionic micelles in self-assembling of fluorescent acridinium-based chemosensors for the detection of mercury (II) ions, J. Photochem. Photobiol. A: Chem. 345 (2017) 74–79.

[7] L. Ding, S. Wang, Y. Liu, J. Cao, Y. Fang, Bispyrene/surfactant assemblies as fluorescent sensor platform: detection and identification of $Cu^{2+}$ and $Co^{2+}$ in aqueous solution, J. Mater. Chem. A 1 (2013) 8866–8875.

[8] L. Ding, Y. Bai, Y. Cao, G. Ren, G. J. Blanchard, Y. Fang, Micelle-Induced Versatile Sensing Behavior of Bispyrene-Based Fluorescent Molecular Sensor for Picric Acid and PYX Explosives, Langmuir 30 (2014) 7645-7653.

[9] N. Dey, S. Bhattacharya, Trace level $Al^{3+}$ detection in aqueous media utilizing luminescent ensembles comprising pyrene laced dynamic surfactant assembly, Dalton Trans. 47 (2018) 2352–2359.

[10] N. Dey, D. Biswakarma, A. Gulyani, S. Bhattacharya, Microenvironment Sensitive Charge-Transfer Dye for Tandem Sensing of Multiple Analytes at Mesoscopic, Interfaces ACS Sustainable Chem. Eng. 6 (2018) 12807-12816.

[11] B. Maiti, N. Dey, S. Bhattacharya, Engaging Dynamic Surfactant Assemblies in Improving Metal Ion Sensitivity of a 1,4,7-Triazacyclononane-Based Receptor: Differential Optical Response for Cysteine and Histidine, ACS Appl. Bio Mater. 2 (2019) 2365-2373.

[12] K. Ki-Hyun, K. Ehsanul, A. J. Shamin, A review on the distribution of Hg in the environment and its human health impacts, J. Hazard. Mater. 306 (2016) 376-385.

[13] S. Chatterjee, S. Sarkar, S. Bhattacharya, Toxic metals and autophagy, Chem. Res. Toxicol. 27 (2014) 1887–900.

[14] E. M. Nolan, S. J. Lippard, Tools and Tactics for the Optical Detection of Mercuric Ion, Chem. Rev. 108 (2008) 3443–3480.

[15] S. Maiti, C. Pezzato, S. Garcia Martin, L. J. Prins, Multivalent interactions regulate signal transduction in a self-assembled $Hg^{2+}$ sensor J. Am. Chem. Soc. 136 (2014) 11288−11291.

[16] F. Songa, C. Yang, X. Shaoa, L. Dua, J. Zhub, C. Kana, A reversible “turn-off-on” fluorescent probe for real-time visualization of mercury(II) in environmental samples and its biological applications, Dyes Pigments 165 (2019) 444–450.

[17] M. Saleem, M. Rafiq, M. Hanif, Organic material based fluorescent sensor for $Hg^{2+}$: a brief review on recent development, J. Fluoresc. 27 (2017) 31‑58.

[18] Y. Ohba, K. Kubo, T. Igarashia, T. Sakurai, Mechanism of the 10-methylacridinium ion-sensitized photooxidation of N,N-dibenzylhydroxylamine and its derivatives in acetonitrile, J. Chem. Soc., Perkin Trans. 2 (2001) 491–493.

[19] A. Albini, S. Spreti, Photooxidation of methylbenzenes and methylnaphthalenes sensitized by cyanoanthracenes, Z. Naturforsch. 41b (1986) 1286‑1292.

[20] O. S. Wolfbeis, W. Trettnak, Fluorescence quenching of acridinium and 6-methoxyquinolinium ions by $Pb^{2+}$, $Hg^{2+}$, $Cu^{2+}$, $Ag^{+}$ and hydrogen sulphide, Spectrochim. Acta, Part A 43 (1987) 405‑408.

[21] M. Berton, F. Mancin, G. Stocchero, P. Tecilla, U. Tonellato, Self-assembling in surfactant aggregates: an alternative way to the realization of fluorescence chemosensors for Cu(II) ions, Langmuir 17 (2001) 7521-7528.

[22] Bettoni, L. Brinchi, T. Del Giacco, R. Germani, S. Meniconi, C. Rol, G. V. Sebastiani, Surfactant effect on titanium dioxide photosensitized oxidation of 4-dodecyloxybenzyl alcohol, J. Photochem. Photobiol. A: Chem. 229 (2012) 53-59.

[23] W. P. Todd, J. P. Dinnocenzo, S. Farid, Efficient photoinduced generation of radical cations in solvents of medium and low polarity, J. Am. Chem. Soc. 113 (1991) 3601-3602.

[24] S. A. Jonker, F. Ariese, J. W. Verhoeven, Cation complexation with functionalized 9-arylacridinium ions: possible applications in the development of cation-selective optical probes, Recl. Trav. Chim. Pays-Bas. 108 (1989) 109-115.

[25] M. A. Chernyavskaya, V. V. Stefanovich, I. A. Sergeeva, A. S. Belova, Antimicrobial and surface-active properties of cationic surfactants based on chloroalkanes and alkylbenzenes, Pharm. Chem. J. 18 (1984) 784–787.

[26] J. You, X. Yu, X. Li, Q. Yan, R. Xie, Enantioselective hydrolysis of long chain α-amino acid esters by chiral sulfur-containing macrocyclic metallomicelles, Tetrahedron: Asymmetry 9 (1998) 1197–1203.

[27] SCM, Theoretical Chemistry, Vrije Universiteit, Amsterdam, 2008, *Http://Www.Scm.Com*.

[28] A. D. Becke, Density-functional exchange-energy approximation with correct asymptotic behavior, Phys. Rev. A 38 (1988) 3098–3100.

[29] C. Lee, W. Yang, R. G. Parr, Development of the Colle-Salvetti correlation-energy formula into a functional of the electron density, Phys. Rev. B 37 (1988) 785–789.

[30] E. Van Lenthe, E. J. Baerends, J. G. Snijders, Relativistic regular two component hamiltonians. J. Chem. Phys. 99 (1993) 4597–4610.

[31] E. Van Lenthe, E. J. Baerends, J. G. Snijders, Relativistic total energy using regular approximations, J. Chem. Phys. 101 (1994) 9783–9792.

[32] E. Van Lenthe, Geometry optimizations in the zero order regular approximation for relativistic effects, J. Chem. Phys. 110 (1999) 8943–8953.

[33] P. Mukerjee, K.J. Mysels, Critical Micelle Concentrations of Aqueous Surfactant System, Superintendent of Documents, U.S. Government Printing Office, Washington, D.C, 1971.

[34] Y. Yan, Y. Hu, G. Zhao, X. Kou, A novel azathia-crown ether dye chromogenic chemosensor for the selective detection of mercury(II) ion, Dyes Pigments 79 (2008) 210−215.

[35] H. Zheng, Z.-H. Qian, L. Xu, F.-F. Yuan, L.-D. Lan, J.-G. Xu, Switching the recognition preference of rhodamine B spirolactam by replacing one atom: design of rhodamine B thiohydrazide for recognition of Hg(II) in aqueous solution, Org. Lett. 8 (2006) 859−861.

[36] S. Basili, T. Del Giacco, F. Elisei, R. Germani, An acridinium-based sensor as a fluorescent photoinduced electron transfer probe for proton detection modulated by anionic micelles, Org. Biomol. Chem. 12 (2014) 6677–6683.

[37] A. Adenier, M. M. Chehimi, I. Gallardo, J. Pinson, N. Vila, Electrochemical oxidation of aliphatic amines and their attachment to carbon and metal surfaces, Langmuir 20 (2004) 8243–8253.

[38] R. A. Bissell, A. P. d. Silva, H. Q. N. Gunaratne, P. L. M. Lynch, G. E. M. Maguire, C. P. McCoy and K. R. A. S. Sandanayake, in Fluorescent PET (Photoinduced Electron Transfer) Sensors, Berlin, 1993.

[39] A. Melchior, E. Peralta, M. Valiente, C. Tavagnacco, F. Endrizzid, M. Tolazzi, Interaction of $d^{10}$ metal ions with thioether ligands: a thermodynamic and theoretical study, Dalton Trans. 42 (2013) 6074–6082.

[40] M. H. Ha-Thi, M. Penhoat, V. Michelet, I. Leray, Highly Selective and Sensitive Phosphane Sulfide Derivative for the Detection of $Hg^{2+}$ in an Organoaqueous Medium, Org. Lett. 9 (2007) 1133–1136.

[41] H. Zheng, Z.-H. Qian, L. Xu, F.-F. Yuan, L.-D. Lan, J.-G. Xu, Switching the recognition preference of Rhodamine B spirolactam by replacing one atom: design of Rhodamine B thiohydrazide for recognition of Hg(II) in aqueous solution, Org. Lett. 8 (2006) 859–861.

[42] M. L. Helm, C. M. Combs, D. G. VanDerveer, G. J. Grant, Homoleptic Group 12 metal complexes of macrocyclic thioethers: the crystal structures of bis(1,4,7-trithiacyclodecane)M(II) perchlorate:M(II)/zinc(II), cadmium(II), mercury(II), Inorg. Chim. Acta 338 (2002) 182–188.

[43] A. Manceau, K. L. Nagy, Dalton Trans. 11 (2008) 1421–1425.

[44] R. C. Dougherty, Temperature and pressure dependence of hydrogen bond strength: A perturbation molecular orbital approach, J. Chem. Phys. 109 (1998) 7372–7378.]

[45] X.-J. Hu, C.-M. Li, X.-Y. Song, D. Zhang, Y.-S. Li, A new $Cu^{2+}$-selective self-assembled fluorescent chemosensor based on thiacalix[4]arene, Inorg. Chem. Commun. 14 (2011) 1632–1635.

[46] P. Pallavicini, Y.A. Diaz-Fernandez, F. Foti, C. Mangano, S. Patroni, Fluorescent sensors for $Hg^{2+}$ in micelles: a new approach that transforms an ON‑OFF into an OFF‑ON response as a function of the lipophilicity of the receptor, Chem. Eur. J. 13 (2007) 178‑187.

[47] A. A. Ensafi, M. Fouladgar, A sensitive and selective bulk optode for determination of Hg(II) based on hexathiacyclooctadecane and chromoionophore V, Sens. Actuators B 136 (2009) 326–331.

[48] S. J. Lee, J. H. Jung, J. Seo, I. Yoon, K.-M. Park, L. F. Lindoy, S. S. Lee, A chromogenic macrocycle exhibiting cation-selective and anion-controlled color change: an approach to understanding structure−color relationships, Org. Lett. 8 (2006) 1641–1643.

[49] H. Lee, H.-S. Lee, J. H. Reibenspies, R. D. Hancock, Mechanism of “turn-on” fluorescent sensors for mercury(II) in solution and its implications for ligand design, Inorg. Chem. 51 (2012) 10904–10915.